Published in final edited form as:
Cancer Res. 2009 June 1; 69(11): 4911–4917. doi:10.1158/0008-5472.CAN-08-2761.

Differentiation of malignant B-lymphoma cells from normal and activated T-cell populations by their intrinsic autofluorescence

Seth M. Pantanelli[1,2,3], **Zhuqing Li**[2], **Robert Fariss**[2], **Sankaranarayana P. Mahesh**[2], **Baoying Liu**[2], and **Robert B. Nussenblatt**[2]

[1]Howard Hughes Medical Institute, Bethesda, MD 20814

[2]National Institutes of Health, Bethesda, MD 20814

[3]University of Rochester School of Medicine and Dentristry, Rochester, NY 14627

Abstract

Patients with active posterior and intermediate uveitis have inflammatory cells in their vitreous; those with primary intraocular lymphoma have malignant B-lymphoma cells concomitantly. These cell types cannot be distinguished clinically. The goal of this study was to investigate intrinsic autofluorescence as a non-invasive way of differentiating immune and lymphomatous cell populations. Human primary T-cells were stimulated with or without anti-CD3 plus anti-CD28 stimulation. B-lymphoma cells (CA46) were cultured separately. Five experimental groups were prepared: unstimulated T-cells, stimulated T-cells, CA46 cells, stimulated T-cells mixed with CA46 cells at a ratio of 1:3, or mixed at a ratio of 3:1. Samples were excited with three wavelengths and imaged with a confocal microscope. For each condition, the autofluorescent emissions from the sample were measured. In separate experiments, T-cells or CA46 cells were injected into the anterior chamber of a Balb/C mouse eye and autofluorescence was measured. Pure T-cell and lymphoma populations were clearly distinguishable based on autofluorescence intensity spectra. CA46 cells were the least fluorescent when excited with 351nm light, but most fluorescent when excited with longer wavelengths like 488nm. Mixed populations of T-cells and CA46 cells had emission intensities that fell predictably in-between those of the pure populations. An ex vivo study demonstrated that CA46 cells could be detected based on their intrinsic autofluorescence. Our studies demonstrated that normal activated and malignant lymphocyte populations can be distinguished based on their intrinsic autofluorescent properties. Future work with in vivo models may prove useful in facilitating the diagnosis of uveitis and other ocular diseases.

Keywords

autofluorescence; primary intraocular lymphoma; primary central nervous system lymphoma; uveitis

Introduction

Primary intraocular lymphoma (PIOL) is a subset of primary central nervous system lymphoma (PCNSL) that first presents clinically in the eye.(1) Other systemic lymphomas metastatic to the eye usually present with additional symptoms like lymphadenopathy, fever, and weight

Correspondence: Robert B Nussenblatt, MD., Building 10 / Room 10S219, 9000 Rockville Pike, Bethesda, MD 20892. Tel: 301-496-3123; Fax: 301-480-1122; Email: DrBob@nei.nih.gov.

Concerning the research or instruments described in this article, Mr. Pantanelli, Dr. Fariss, Dr. Li, Dr. Mahesh, Dr. Liu, and Dr. Nussenblatt have no proprietary interest.

loss, which facilitates diagnosis. Alternatively, the most common initial complaint from patients later diagnosed with PIOL are floaters.(2–4) These non-specific symptoms often delay diagnosis months or even years.(5)

The challenge in diagnosing PIOL comes from its clinical similarity to chronic non-infectious inflammatory disease.(6) While benign processes (i.e. sarcoidosis, Behcet's disease) present with an array of inflammatory cells in the vitreous, patients with PIOL are known to have a mixture of both malignant B-cells and reactive T-cells in the vitreous. Since the clinical examination prevents differentiating between these two entities, more invasive tests are often required. Ancillary tests can be useful but none are definitive in making the diagnosis; as a result a diagnostic vitrectomy is often performed.(7) Even a vitrectomy is not completely diagnostic, since lymphoma cells are delicate and may easily degenerate in the vitreous.(8–10) When these methods fail, ocular tissue biopsy or enucleation might be required to confirm the diagnosis.(11)

Other methods to aid in the diagnosis of PIOL have been attempted. In 1995, Chan et. al. published a prospective comparative case series that identified increased levels of interleukin-10 (IL-10) in the vitreous of patients with PIOL when compared to benign endogenous or infectious uveitis.(12) Buggage et. al. further clarified this finding in 1999 by demonstrating that an IL-10 to IL-6 ratio greater than 1.0 might be more diagnostic.(13) However, the technique is based on an invasive procedure, a vitrectomy.

Recently, Li et. al. published work on the first murine B-cell intraocular lymphoma model for PIOL. In their study they used a human B-lymphoma cell line (CA46) that expressed CD22, CXCR4, CXCR5, and IL-10, characteristics typically noted in PIOL cells.(14) When these cells were injected into the eyes of SCID mice, histology at day 10 showed persistence of lymphoma cells in the vitreous as well as colonization and invasion into the retina. The model mimicked human PIOL in that it also preferentially invaded and expanded into the subretinal space and was shown to metastasize to the CNS at a later stage. Their work provides a unique model for exploring new diagnostic techniques for human PIOL.

Autofluorescence is a natural property of living cells whereby endogenous fluorophores emit light when excited with light of a shorter wavelength. It is a natural phenomenon that is attractive to study as a potential diagnostic tool because it can be used safely, noninvasively, and quickly for characterizing the metabolic and phenotypic properties of living tissue. In 1987, Alfano et. al. showed that fluorescence spectroscopy could be used to differentiate between normal and malignant human breast tissues.(15) Since then, many others have demonstrated clinical utility in the diagnosis of breast (16), lung (17), and esophageal cancers (18). Progress by Monici and Heintzelman has also been made characterizing the autofluorescence of white blood cells, though the clinical applications are not yet as apparent.(19,20)

As it pertains to the eye, autofluorescence of the retina is already used clinically as a prognostic indicator for age-related macular degeneration (AMD).(21) Attempts have not yet been made to use autofluorescence in the vitreous or anterior chamber to differentiate between normal and malignant cells floating in eyes with cellular infiltrates. However, the differences in these cell populations should be established *in vitro* before tackling the obstacles associated with measuring these cells *in vivo* (i.e. eye movement, attenuation of AF signal by cornea). The purpose of this study was to investigate whether autofluorescence could be used to distinguish between normal and malignant cell populations, namely activated T-cells and a malignant human B-lymphoma cell line (CA46).

Materials and Methods

T-cell purification and culture

Peripheral blood mononuclear cells (PBMCs) were isolated from normal human donor buffy coat blood products as described previously.(22) T-cells were then isolated from PBMCs using magnetic bead separation (Pan T-cell Isolation Kit II; Miltenyi Biotec, Auburn, CA). The T-cells were divided into two groups, resting and stimulated. The stimulated T-cells were treated with anti-human CD3 and CD28 antibodies (BD Bioscience, San Jose, CA) at a concentration of 2 μg/ml and were incubated at 37 degrees for 30 minutes. Both the resting and stimulated T-cells were cultured at a concentration of 2×10^6 cells/ml at 37°C and 5% CO_2 in culture medium [RPMI 1640 with 10% fetal bovine serum, 1x antibiotics (penicillin and streptomycin), and 2 mM glutamine].

CA46 cell line culture

The human B-lymphoma cell line (CA46) was obtained from American Type Culture Collection (Mannasas, VA). When cultured, CA46 cells were cultured at 37°C in the same medium described above for T-cells and cell density was strictly maintained between 2×10^5 and 6×10^5 / ml at all times. CA46 cells entered their exponential phase of growth before imaging studies began (approximately 4 days after thawing), and all imaging studies were complete on or prior to passage 4.

Preparation of in-vitro samples

Resting T-cells, stimulated T-cells, and CA46 cells were washed and resuspended in PBS at a concentration of 2×10^6 / ml. Five experimental groups were prepared: resting T-cells, stimulated T-cells, stimulated T-cells mixed with CA46 cells at a ratio of 1:3 or 3:1, and CA46 cells. About 6×10^5 cells cells were cyto-spun onto microscope slides. Slides were immediately removed from the centrifuge, cover-slipped with PBS, and sealed. Imaging was carried out within two-hours of centrifugation. A separate trypan blue staining showed that greater than 95% of all cells were still viable immediately following and 1 hour after centrifugation onto the slides.

Autofluorescence measurement and analysis for in-vitro samples

All autofluorescence imaging was done using a Leica SP2 confocal microscope. For *in vitro* imaging, a 40x oil immersion objective was used. When exciting with 351 nm light, emissions from the sample passed through an acousto-optical beam splitter to the photomultiplier tube (PMT). Only pure resting T-cell and CA46 cell populations were measured zero and one day after isolation. When the samples were excited with 458 and 488 nm light, a dichroic beam splitter (Chroma Qdot filter Z488RDC) filtered light coming from the sample but had greater than 90% transmission of light from 512 nm to 600 nm. For each sample, a field was selected that contained less than 5% debris and greater than 95% confluent cells.

Using the Leica confocal software package, multiple regions of interest (ROI) were defined within the chosen field. A differential interference contrast (DIC) image was first taken so that the origin of autofluorescent signals could be confirmed. An example of one such image is shown in Figure 1. To measure autofluorescence, the field was illuminated with 3 different excitation wavelengths (351, 458, and 488 nm). For each excitation condition, the sample was scanned in 5 nm increments over a broad range of emissions wavelengths. When samples were excited with 351 nm light, scanning occurred from 400–600 nm; when exciting with 458 or 488, scanning occurred from 512–600 nm. The intensity versus wavelength measurements from the ROIs were averaged to give a final, single autofluorescence spectral profile for that sample and excitation condition.

In a separate experiment, CA46 cells and T-cells that had been stimulated with anti-human CD3 and CD28 antibodies for 3 days were excited with the 488 nm light as described above; however, instead of measuring emissions in 5 nm increments, the total emission from a broad range of wavelengths (520–580 nm) was quantified in a single measurement. Regions of interest were drawn around 10 individual cells from each field. This was used to investigate whether the two populations could be distinguished based on a limited number of cells.

Preparation of ex-vivo samples

One challenge when imaging cells *ex vivo* is physically locating the cells within the three dimensional chamber (eye) that they are suspended in. To facilitate locating the cells in the eye, stimulated T-cells and CA46 cells were stained with DAPI (4',6-diamidino-2-phenylindole) prior to being imaged. This stain was carefully chosen because of its unique excitation / emission profile. When DAPI is excited with light ranging in wavelength between 300 and 425 nm, it characteristically fluoresces between 380 and 600 nm. However, it does not fluoresce when excited with light greater than 425 nm. Therefore, UV excitations at 351 nm were used to detect the DAPI signal and locate cells *ex vivo*, while visible 488 nm light was used to generate the same autofluorescent signals seen *in vitro* between 500 and 600 nm.

To verify that fixation and DAPI staining described above would not interfere with autofluorescence measurements at 488 nm excitation. On the day of imaging (2 days after T-cell stimulation), normal stimulated T-cells and CA46 cells were washed and resuspended in a fixation buffer (medium A; Caltag Laboratories, Burlingame, CA) followed by incubation at room temperature for 10 minutes with permeabilization buffer (medium B; Caltag Laboratories, Burlingame, CA). Samples were either left unstained or stained with DAPI at a concentration of 1 μg / ml at room temperature for 10 minutes, washed, and resuspended in PBS at a final concentration of 50×10^6 cells / ml. A separate experiment confirmed that DAPI staining of T-cells and CA46 cells was 100% efficient when using the method described above.

Cells set aside for unstained and stained controls were prepared and imaged exactly as described above for the *in vitro* experiments. The purpose of the slides was to demonstrate that the DAPI staining had no effect on autofluorescence of T-cells and CA46 cells when excited with visible 488 nm light. The remaining stained T-cells and CA46 cells suspended in PBS at a concentration of 50×10^6 / ml were injected (2 μl) into the anterior chambers of Balb/C mice under the direction of a fundoscopy to ensure that the injection was successful and that the injected cells were well dispersed throughout the anterior chamber. The mice were euthanized less than 5 minutes before imaging began, and no measurements were taken longer than 40 minutes after euthanization.

Autofluorescence measurement and analysis for ex-vivo samples

The Balb/C mouse was placed directly under the microscope objective immediately following euthanization. All *ex vivo* imaging used a 20x dipping objective with a working distance of 3.5mm. Water was carefully added so that it provided a continuous path for the light between the objective and the cornea. This ensured that the cornea remained moist for the duration of the experiment; it also optically negated most of the focusing power of the cornea, since both the cornea and water have similar refractive indices (1.40 vs. 1.33).(23) First, the field was illuminated with 351 nm light and the anterior chamber was scanned for clusters of floating cells. For each field of interest, one picture was captured with 351 nm excitation and a second picture was captured with 488 nm excitation. When 488 nm light was used, autofluorescent signals were measured between 520 and 580 nm. For autofluorescent images captured with 488 nm excitation, the signal to noise ratio was increased by capturing an accumulated image (i.e. by overlaying multiple images of the same field).

Data analysis and statistics

Emission curves were generated by measuring the average intensity from each ROI at 5 nm increments along the emission range of interest. Curves were further smoothed by averaging all measured ROIs for a particular sample. As a result, each emission curve is the result of measuring between 200–1000 cells from each population. Error bars on each curve (Fig. 2) represent one standard deviation away from the mean at that data point. The students' t-test was used to compare peak emission intensities from different populations. A p-value less than 0.01 was used to claim statistical significance.

Spectral analysis (Table 1) involved calculating the ratio of emission intensities at specific wavelengths, given an appropriate excitation wavelength. It is well documented in the literature that the free and bound forms of NAD(P)H fluoresce at 465 and 445 nm, respectively, when excited with 350 nm light, and that the flavin coenzymes (i.e. FAD) fluoresce at approximately 520 nm when excited with 450 nm light.(18,24) Therefore, the 445/465 ratio acts as a surrogate measure of free vs. bound NAD(P)H and 445/520 and 465/520 ratios act as surrogate measures of NAD(P)H vs. flavin concentration.

Results

The results of characterizing the autofluorescence of the five groups of cells described earlier are presented in Figure 2. For samples excited with 351 nm light, emissions are shown for resting T-cells and CA46 cells and 0 and 1 day after isolation. For 458 and 488 nm excitation sources, emissions are shown after 0, 1, and 3 days of incubation. In Figure 2a, the cell populations were excited with 351 nm light and autofluorescent emissions were measured between 400 and 600 nm. In figures 2b and 2c, the cell populations were excited with 458 and 488 nm light, respectively, and emissions were recorded between 512 and 600 nm. On the first day of imaging (t = 0 days), only four groups were imaged since it was assumed that there would be no difference between resting cells and cells that had been stimulated that same day.

Resting and stimulated T-cells can be differentiated based on autofluorescence intensity differences *in* vitro

When stimulated and resting T-cells were excited with visible wavelengths (figs. 2b and 2c), differences between the two populations were small and insignificant at 458 ($p = 0.12$) and 488 ($p = 0.17$) nm excitation one day after stimulation (t = 1 day). However, after three days of stimulation, resting and stimulated T-cells differed dramatically in their fluorescence emission intensities, regardless of the excitation wavelength ($p < 0.001$). Stimulated T-cells were more intensely fluorescent than resting T-cells by a factor of 1.3 when excited with 458 nm light, and by a factor of 1.6 when excited with 488 nm light. These ratios were obtained by dividing the maximum emission intensity of the stimulated T-cells by the maximum emission intensity achieved by the resting T-cells.

Resting and stimulated T-cell autofluorescence dramatically differs from that of CA46 cell autofluorescence when excited with both UV and visible light *in vitro*

As shown in Figure 2a, resting T-cells fluoresced more intensely that CA46 cells when excited with UV light (351 nm), regardless of the number of days after isolation (i.e. t = 0 or 1 days). Resting T-cell populations had peak fluorescence intensities at 490 ± 5 nm. Although CA46 cells also had a peak emission at 490 nm, they appeared instead to autofluoresce weakly over a broad spectrum ranging from 400 to 600 nm. At t = 0 days, resting T-cells autofluoresced with a peak intensity 1.7 times that of the CA46 cells. Although this difference narrowed 1 day after incubation, statistically significant differences were maintained throughout ($p < 0.0001$).

When 458 and 488 nm excitation was used, all populations of cells exhibited fluorescence with peak intensities at 535 ± 5 nm. In contrast to that seen in Fig. 2a, figures 2b and 2c show that CA46 cells were considerably more intense than resting and stimulated T-cells when excited with visible wavelengths. CA46 cells were 1.7 ($p < 0.0001$) and 1.58 ($p < 0.0001$) times more intense than stimulated T-cells at 1 and 3 days after stimulation, respectively, when excited with 458 nm light. Differences between stimulated T-cells and CA46 cells were slightly smaller when excited with 488 nm light, however they were always statistically significant ($p \leq 0.0006$). Since resting T-cells were almost equal to or less than stimulated T-cells in terms of fluorescence when excited with visible wavelengths, the differences between resting T-cells and CA46 cells were similar to those described above with stimulated T-cells.

Results from above required measuring the average intensity from large regions of interest that contained hundreds of cells. Since, clinically, the number of cells floating in the eyes of patients with uveitis or primary intraocular lymphoma may be below 20,000, we wanted to investigate whether the differences could still be detected when measurements were based on a small number of cells. In a separate experiment, CA46 cells and T-cells that had been stimulated for 3 days were excited with the 488 nm excitation light and the total emission from a broad range of wavelengths (520–580 nm) was quantified in a single measurement. Regions of interest were drawn only around individual cells. The results are shown in Figure 3. Although autofluorescence was measured from 10 cells from each population, signal from only 8 cells was adequate to differentiate them. CA46 cells were approximately 1.8 times more fluorescent than stimulated T-cells, and this difference was statistically significant ($p = 0.003$).

Mixtures of CA46 cells and T-cells fell predictably in between spectra derived from pure T-cell and CA46 cell populations

Clinically, PIOL patients will most certainly present with a mixture of B-lymphoma and activated T-cells floating in the vitreous. As such, we wished to establish that: 1) such mixtures would have predictable fluorescence intensity characteristics in-between that of pure populations described above, and 2) that they could be distinguished from pure T-cell populations, which has value clinically. Two mixtures were studied: activated T-cells and CA46 cells mixed at a ratio of 1:3, and at a ratio of 3:1. At $t = 0$, the mixtures included resting instead of activated T-cells. Results are included in Figure 2.

In Fig. 2b, the mixtures were of CA46 and stimulated T-cells were distinguishable at $t = 0$ ($p = 0.0007$), $t = 1$ ($p = 0.0086$), and $t = 3$ ($p = 0.0005$) days of stimulation. Mixtures containing CA46 cell to T-cell ratios of 3:1 were more fluorescent than those containing ratios of 1:3, as expected. In Fig. 2c, mixtures of CA46 cells and T-cells were only distinguishable from each other at $t = 0$ ($p = 0.0063$); however, mixtures containing CA46 cell to T-cell ratios of 3:1 were always more fluorescent than those containing 1:3, which is exactly what was expected.

When excited with 458 nm light, resting T-cells were significantly less fluorescent than mixtures of CA46 and T-cells at $t = 0$ ($p < 0.002$). One and three days after stimulation, activated T-cells could still easily be distinguished from the mixtures ($p < 0.003$). Although the same trends also held when cells were excited with 488 nm light, differences were not large enough to be statistically significant ($p \geq 0.01$).

Autofluorescence of T-cells and CA46 cells can be detected *ex vivo*

In vitro controls were used to compare autofluorescence of unstained and DAPI stained cells excited with 488 nm light. The results of this experiment are shown in Figure 4. When both stained and unstained stimulated T-cells were excited with 351 nm light, the DAPI stained cells brightly fluoresced and were clearly identifiable; unstained cells autofluoresced faintly, as expected. When the exact same fields were excited with 488 nm light, both stained and

unstained stimulated T-cells fluoresced similarly. Autofluorescence was objectively measured exactly as described for the *in vitro* experiments; both sets of cells had nearly identical emission intensity vs. wavelength profiles. This substantiated the assumption that any signal seen *ex vivo* was not being augmented by the presence of DAPI stain. A separate experiment also confirmed that there was no difference in autofluorescence intensity spectra of fixed (paraformaldehyde) and non-fixed cells.

The results of imaging CA46 cells *ex vivo* are shown in Figure 5. In Figure 5a, the CA46 cells were found floating in the anterior chamber by exciting the field with 351 nm light. In Figure 5b, the same cells are shown when excited with 488 nm light. Sixteen frames were acquired to generate an accumulated image; this increased the signal to noise ratio. The signal seen in Fig. 5b is due to autofluorescence.

Discussion

We have characterized the autofluorescent properties of resting and stimulated T-cells, as well as malignant human B-lymphoma (CA46) cells. To the best of our knowledge, this is the first report to characterize the autofluorescence of T-cells as an isolated population, and also the first time fluorescence measurements have been made on this population over a time-course coincident with stimulation. The results of the *in vitro* work presented here established that resting and activated T-cells can be differentiated on the basis of autofluorescence intensity 3 days after stimulation. This finding, by itself, may have value clinically when evaluating patients with chronic vitreitis. It is not currently known what proportion of T-cells are resting or activated in patients with any form of vitreitis, though it is assumed that activated T-cells are more highly associated with active disease. The ability to measure relative concentrations of resting and activated T-cells non-invasively may serve as a prognostic indicator for the underlying disease, objectively establish the severity, help to establish whether the patient is in a pre-clinical active or remissive state, or assess the efficacy of treatment.

The results above also establish that normal as well as activated T-cells and CA46 cells can be differentiated based on autofluorescence intensity. We have shown that these differences can be determined by measuring signal from as few as 8 cells, which has important implications for applying this technology as a diagnostic tool. As emphasized earlier, most diagnostic tests currently used for PIOL either lack sensitivity or are extremely invasive and carry with them additional risks (i.e. sympathetic ophthalmia). Using autofluorescence as an aid in diagnosis may significantly decrease the morbidity associated with other diagnostic procedures. As a proof of concept, we have also shown that autofluorescent signals can be detected from within the anterior chamber of a mouse eye.

Our results from excitation with UV light are consistent with previous work. As noted above, when all of the cell populations studied here were excited with 351 nm light, they exhibited emissions with peak intensities at 490 nm. Many others including Villette (18), Monici (20), and Pradhan (25) described emission peaks between 440 and 490 nm when exciting with 350 nm light, and they ascribed this finding to the autofluorescence of nicotinic coenzymes (NAD(P)H). It should be noted that our results are similar to those previously published despite our use of an entirely different imaging modality; namely, confocal microscopy in our study and spectrofluoroscopy in others.

Results from this study involving visible excitations (456 and 488 nm) are also extremely consistent with previous work. In Heintzelman's study of leukocytes and cervical epithelial cancer cells, a strong peak at 530 nm was observed when exciting with 450 nm light.(19) This is nearly identical to what was found in this study - when resting and stimulated T-cells or CA46 cells were excited with 458 nm light, emission was seen with a peak intensity at 535

nm. Heinzelman also noted an emission at 530 nm in a minority of neutrophils with excitation at 500 nm; this may in fact be synonymous with the 535 nm peak seen in this study when all populations were excited with 488 nm light. As others have already suggested, cell autofluorescence in the 500–560 nm range is thought to be due to emission from flavins and flavin coenzymes. (26,27)

To better understand the biochemical roots of the observed AF differences, we calculated intensity ratios for emission wavelengths that are known to correspond with the concentration of free and bound NAD(P)H (465 nm and 445 nm) and flavin coenzymes (520 nm). The results of this spectral analysis are presented in Table 1. When comparing T-cells and CA46 cells, there was a significant difference in the 445/465 ratio for T-cells and CA46 cells at t = 0; however, this difference decreased the next day, after resting T-cells had been left in culture for 24 hours. Perhaps more interesting are the differences between T- and CA46 cells with regards to the 445/520 and 465/520 ratios. CA46 cells maintained lower ratios at t = 0 and t = 1 day when compared to T-cells. Since this suggests a higher concentration of flavins in the CA46 cells, one can conclude that these cells had an enhanced level of aerobic metabolism over all time periods considered when compared to T-cells. It is interesting to note that the increased aerobic metabolism is in contrast to what has been observed in another neoplastic cell line by Croce et al.(28)

Over time, CA46 cells had increasing 445/520 and 465/520 ratios (from t = 0 to t = 1 day), indicating a depletion of oxidized flavins with cell splitting and increased passage number. Since aerobic metabolism decreased over time and the rate of cell division remained the same or increased, anaerobic metabolism must have proportionately increased. This is consistent with what has been observed in many other cell lines – namely, that cells in their exponential phase of growth experience a shift toward anaerobic metabolism with time since thawing and number of passages. (24,28) In contrast to the above, T-cell flavin ratios actually decreased over time, indicating that aerobic metabolism was likely enhanced over the observed period. Although there are no correlates in the literature to explain this phenomenon, it is possible that resting T-cells regulated and enhanced their aerobic energy metabolism as they *entered* an exponential growth phase.

To improve sensitivity of measuring autofluorescence *ex vivo*, we suggest several modifications to the above described methods. In this study, *ex vivo* imaging was done on cells that were fixed prior to injection into the anterior chamber. Although a separate experiment in our study confirmed that this fixation did not affect AF intensity, some suggest that fixation can alter (and often increase) the autofluorescence of cells. Therefore, hardware and software enhancements may be required to increase the signal to noise ratio as attempts are made to image these cells in a human eye. We also found that careful choice of a microscope objective that has a long working distance (for imaging through the cornea and lens) and excellent transmission properties in the light range of interest (400–600 nm) is critical to maximizing image quality. Alternatively, two-photon microscopy may be better suited for *in vivo* imaging due to its penetration depth. In addition, new imaging technologies like adaptive optics (AO) paired with confocal laser scanning ophthalmoscopy may help to compensate for the eyes aberrations and provide higher signal to noise ratios.(29) Using eye tracking or advanced software algorithms capable of compensating for eye movements would be necessary to bring this technology to the clinic.

Conclusions

The intrinsic fluorescence of both normal T-cells and a malignant human B-lymphoma cell line (CA46) was studied. We have concluded that the two populations can be differentiated based upon their emissions when excited with wavelengths including 351, 458, and 488 nm.

This difference can be detected by characterizing the autofluorescence signal from as few as 8 cells. Spectral analysis shows that the CA46 cells have a relative increase in aerobic energy metabolism compared to T-cells (under the conditions tested); this dissimilarity underpins the intensity differences that allow for cell-type differentiation. We have also shown that the autofluorescent emissions can be detected from within the anterior chamber of a Balb/C mouse eye. Future work that combines enhanced imaging modalities like two-photon imaging with sophisticated image analysis may ultimately allow translation to the clinic.

Acknowledgement

This research was funded by the intramural research program at the National Eye Institute and the Howard Hughes Medical Institute.

Non-standard abbreviations

PIOL, primary intraocular lymphoma
MRI, magnetic resonance imaging
CSF, cerebrospinal fluid
PCNSL, primary central nervous system lymphoma
IL-10, interleukin-10
AMD, age-related macular degeneration
PBMC, peripheral blood mononuclear cells
ROI, region of interest
DIC, differential interference contrast
AO, adaptive optics
OCT, optical coherence tomography

References

1. Nussenblatt, RB.; Whitcup, SM. Uveitis. Vol. Third Edition. 2004.
2. Akpek EK, Ahmed I, Hochberg FH, et al. Intraocular-central nervous system lymphoma: clinical features, diagnosis, and outcomes. Ophthalmology 1999;106:1805–1810. [PubMed: 10485554]
3. Buggage RR, Chan CC, Nussenblatt RB. Ocular manifestations of central nervous system lymphoma. Curr Opin Oncol 2001;13:137–142. [PubMed: 11307054]
4. Freeman LN, Schachat AP, Knox DL, Michels RG, Green WR. Clinical features, laboratory investigations, and survival in ocular reticulum cell sarcoma. Ophthalmology 1987;94:1631–1639. [PubMed: 3323986]
5. Whitcup SM, de Smet MD, Rubin BI, et al. Intraocular lymphoma. Clinical and histopathologic diagnosis. Ophthalmology 1993;100:1399–1406. [PubMed: 8371930]
6. Cassoux N, Merle-Beral H, Leblond V, et al. Ocular and central nervous system lymphoma: clinical features and diagnosis. Ocul Immunol Inflamm 2000;8:243–250. [PubMed: 11262654]
7. Nasir S, DeAngelis LM. Update on the management of primary CNS lymphoma. Oncology (Williston Park) 2000;14:228–234. [PubMed: 10736810]discussion 37–42, 44.
8. Karma A, von Willebrand EO, Tommila PV, Paetau AE, Oskala PS, Immonen IJ. Primary Intraocular Lymphoma Improving the Diagnostic Procedure. Ophthalmology. 2007
9. Whitcup SM, Chan CC, Buggage RR, Nussenblatt RB, Byrnes GA, Rubin BI. Improving the diagnostic yield of vitrectomy for intraocular lymphoma. Arch Ophthalmol 2000;118:446. [PubMed: 10721983]
10. Coupland SE, Bechrakis NE, Anastassiou G, et al. Evaluation of vitrectomy specimens and chorioretinal biopsies in the diagnosis of primary intraocular lymphoma in patients with Masquerade syndrome. Graefes Arch Clin Exp Ophthalmol 2003;241:860–870. [PubMed: 14605902]
11. Levy-Clarke GA, Byrnes GA, Buggage RR, et al. Primary intraocular lymphoma diagnosed by fine needle aspiration biopsy of a subretinal lesion. Retina 2001;21:281–284. [PubMed: 11421029]
12. Chan CC, Whitcup SM, Solomon D, Nussenblatt RB. Interleukin-10 in the vitreous of patients with primary intraocular lymphoma. Am J Ophthalmol 1995;120:671–673. [PubMed: 7485372]

13. Buggage RR, Whitcup SM, Nussenblatt RB, Chan CC. Using interleukin 10 to interleukin 6 ratio to distinguish primary intraocular lymphoma and uveitis. Investigative ophthalmology & visual science 1999;40:2462–2463. [PubMed: 10476821]

14. Li Z, Mahesh SP, Shen de F, et al. Eradication of tumor colonization and invasion by a B cell-specific immunotoxin in a murine model for human primary intraocular lymphoma. Cancer Res 2006;66:10586–10593. [PubMed: 17079483]

15. Alfano RR, Tang GC, Pradhan A, Lam W, Choy DSJ, Opher E. Fluorescence-Spectra from Cancerous and Normal Human-Breast and Lung Tissues. Ieee Journal of Quantum Electronics 1987;23:1806–1811.

16. Gupta PK, Majumder SK, Uppal A. Breast cancer diagnosis using N2 laser excited autofluorescence spectroscopy. Lasers Surg Med 1997;21:417–422. [PubMed: 9365951]

17. Pitts JD, Sloboda RD, Dragnev KH, Dmitrovsky E, Mycek MA. Autofluorescence characteristics of immortalized and carcinogen-transformed human bronchial epithelial cells. J Biomed Opt 2001;6:31–40. [PubMed: 11178578]

18. Villette S, Pigaglio-Deshayes S, Vever-Bizet C, Validire P, Bourg-Heckly G. Ultraviolet-induced autofluorescence characterization of normal and tumoral esophageal epithelium cells with quantitation of NAD(P)H. Photochem Photobiol Sci 2006;5:483–492. [PubMed: 16685326]

19. Heintzelman DL, Lotan R, Richards-Kortum RR. Characterization of the autofluorescence of polymorphonuclear leukocytes, mononuclear leukocytes and cervical epithelial cancer cells for improved spectroscopic discrimination of inflammation from dysplasia. Photochemistry and photobiology 2000;71:327–332. [PubMed: 10732451]

20. Monici M, Pratesi R, Bernabei PA, et al. Natural fluorescence of white blood cells: spectroscopic and imaging study. J Photochem Photobiol B 1995;30:29–37. [PubMed: 8558361]

21. Schmitz-Valckenberg S, Bindewald-Wittich A, Dolar-Szczasny J, et al. Correlation between the area of increased autofluorescence surrounding geographic atrophy and disease progression in patients with AMD. Investigative ophthalmology & visual science 2006;47:2648–2654. [PubMed: 16723482]

22. Li Z, Mahesh SP, Kim BJ, Buggage RR, Nussenblatt RB. Expression of glucocorticoid induced TNF receptor family related protein (GITR) on peripheral T cells from normal human donors and patients with non-infectious uveitis. Journal of autoimmunity 2003;21:83–92. [PubMed: 12892739]

23. Patel S, Marshall J, Fitzke FW 3rd. Refractive index of the human corneal epithelium and stroma. J Refract Surg 1995;11:100–105. [PubMed: 7634138]

24. Monici M, Basile V, Romano G, et al. Fibroblast autofluorescence in connective tissue disorders: a future tool for clinical and differential diagnosis? J Biomed Opt 2008;13:054025. [PubMed: 19021405]

25. Pradhan A, Pal P, Durocher G, et al. Steady state and time-resolved fluorescence properties of metastatic and non-metastatic malignant cells from different species. Journal of photochemistry and photobiology 1995;31:101–112.

26. Aubin JE. Autofluorescence of viable cultured mammalian cells. J Histochem Cytochem 1979;27:36–43. [PubMed: 220325]

27. Benson RC, Meyer RA, Zaruba ME, McKhann GM. Cellular autofluorescence--is it due to flavins? J Histochem Cytochem 1979;27:44–48. [PubMed: 438504]

28. Croce AC, Spano A, Locatelli D, Barni S, Sciola L, Bottiroli G. Dependence of fibroblast autofluorescence properties on normal and transformed conditions. Role of the metabolic activity. Photochem Photobiol 1999;69:364–374. [PubMed: 10089830]

29. Liang J, Williams DR, Miller DT. Supernormal vision and high-resolution retinal imaging through adaptive optics. Journal of the Optical Society of America 1997;14:2884–2892. [PubMed: 9379246]

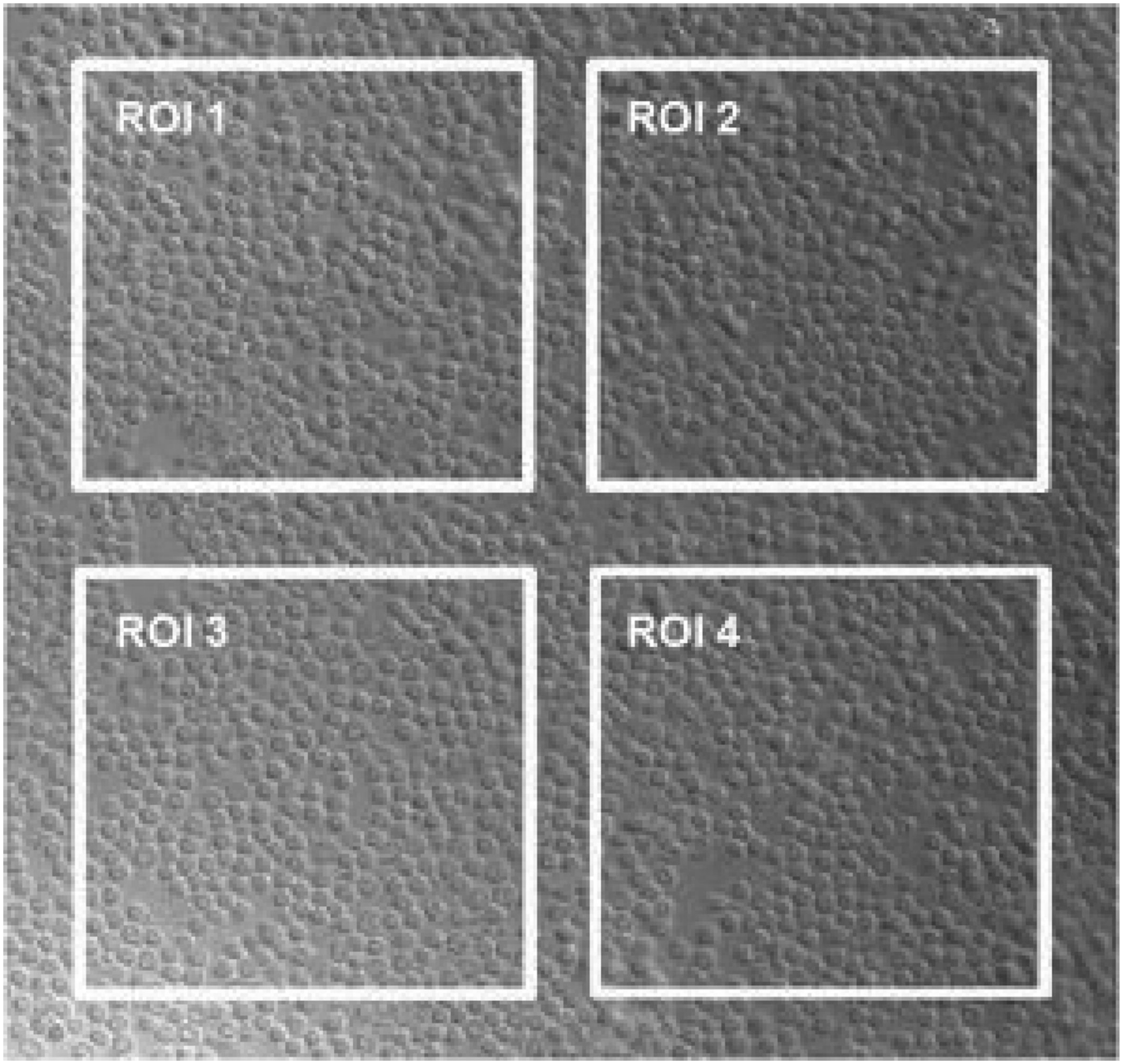

Figure 1. Differential interference contrast (DIC) image of normal resting T-cells

T-cells (0.6×10^6) were cyto-spun onto slides so that they were greater than 95% confluent. A field was selected that was absent of debris, and four regions of interest (ROI) were selected over which autofluorescent intensity could be measured. Note that for simplicity, all ROIs are of equal size and shape. However, all sizes and shapes can be chosen and directly compared to one another since the reported measure is an average intensity defined over the entire ROI.

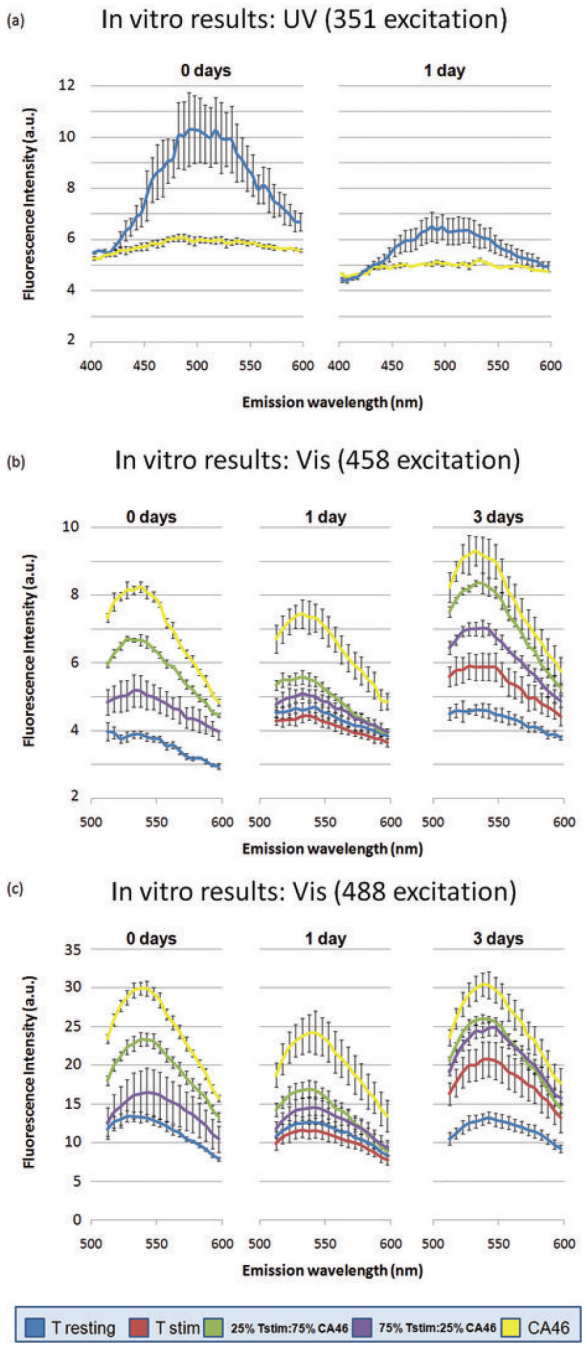

Figure 2. Autofluorescence of malignant B-cells, resting T-cells, and activated T-cells after excitation with UV and visible light

When all populations were excited with UV light (351nm), T-cells were consistently more fluorescent than B-cells (a). When excited with visible wavelengths (458 and 488nm) malignant B-cells fluoresced much more intensely than resting and activated T-cells (b and c). Mixed populations of T- and B-cells had autofluorescence patterns that fell predictably in-between those of the pure populations.

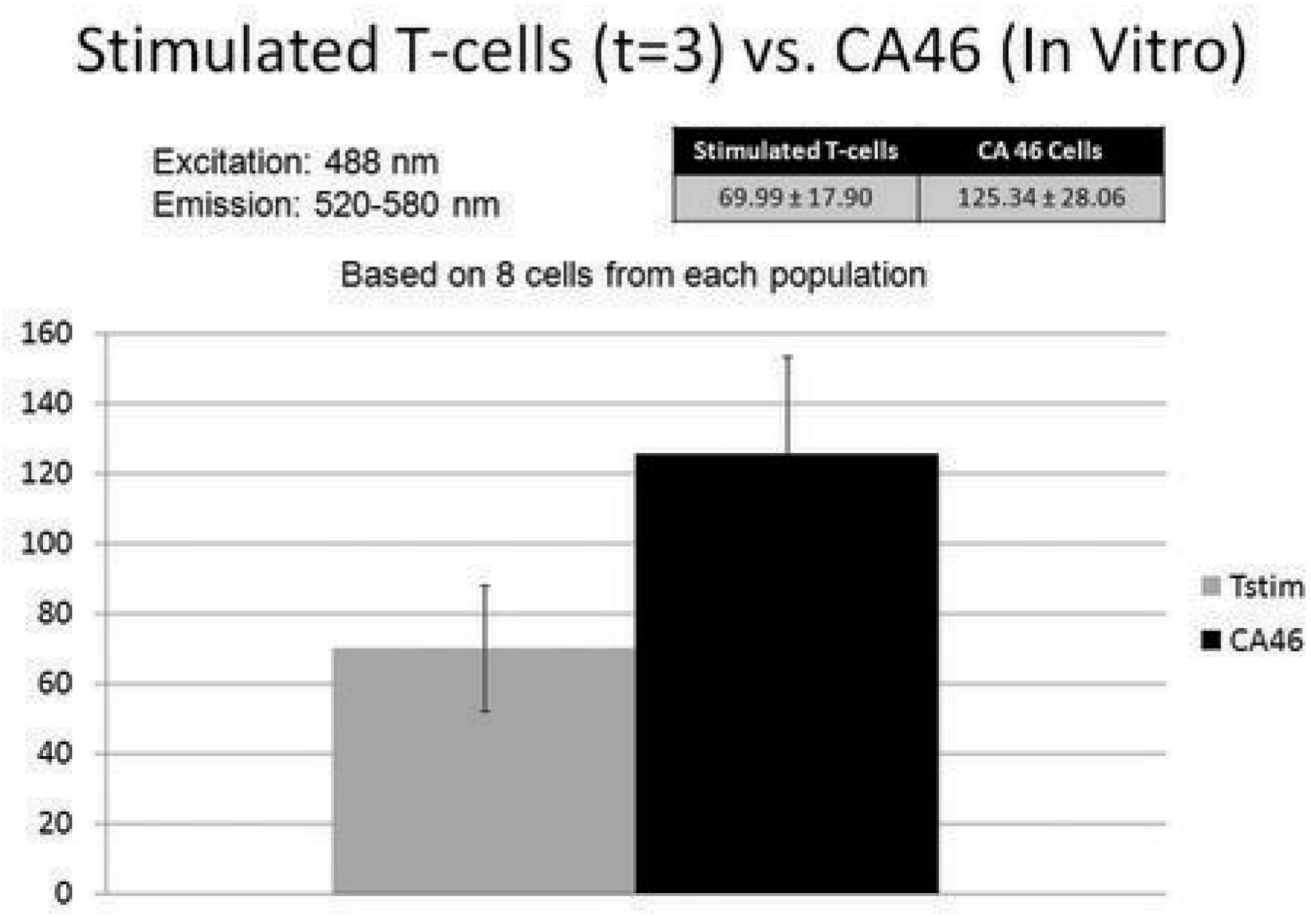

Figure 3. Autofluorescence of stimulated T-cells and malignant B-cells (CA46)

Stimulated T-cells and CA46 cells were separately stimulated with 488 nm light and emissions were measured over wavelengths ranging from 520 to 580 nm. The two populations of cells were clearly distinguished from one another using this method. Averaged signal data from as few as 8 cells was required to make this determination.

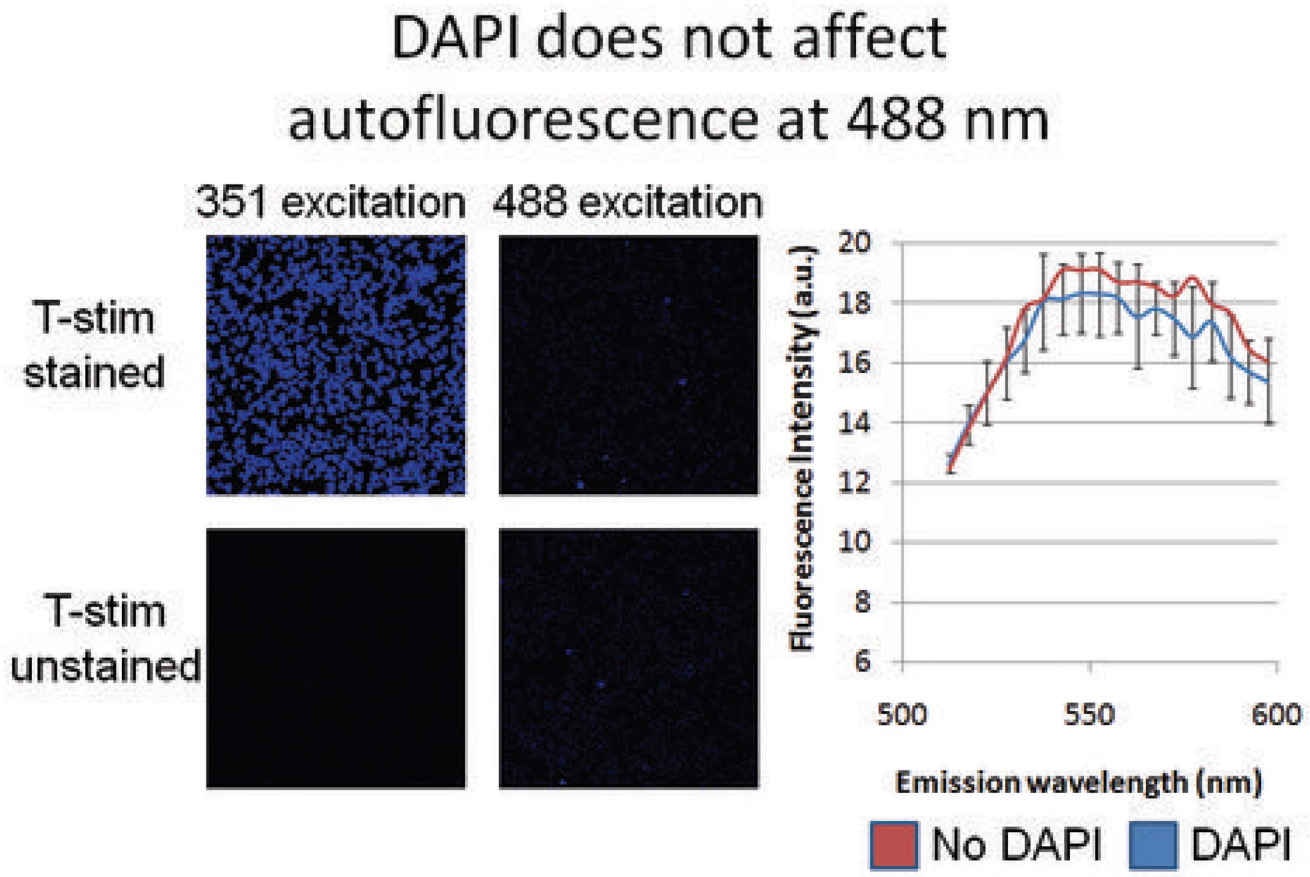

Figure 4. Effect of DAPI on autofluorescence of stimulated T-cells

Stimulated T-cells were stained with DAPI and compared with a population of unstained stimulated T-cells. When excited with 488 nm light, the stained and unstained populations did not differ in florescence characteristics, demonstrating that DAPI does not influence the autofluorescence of cells excited with 488 nm light.

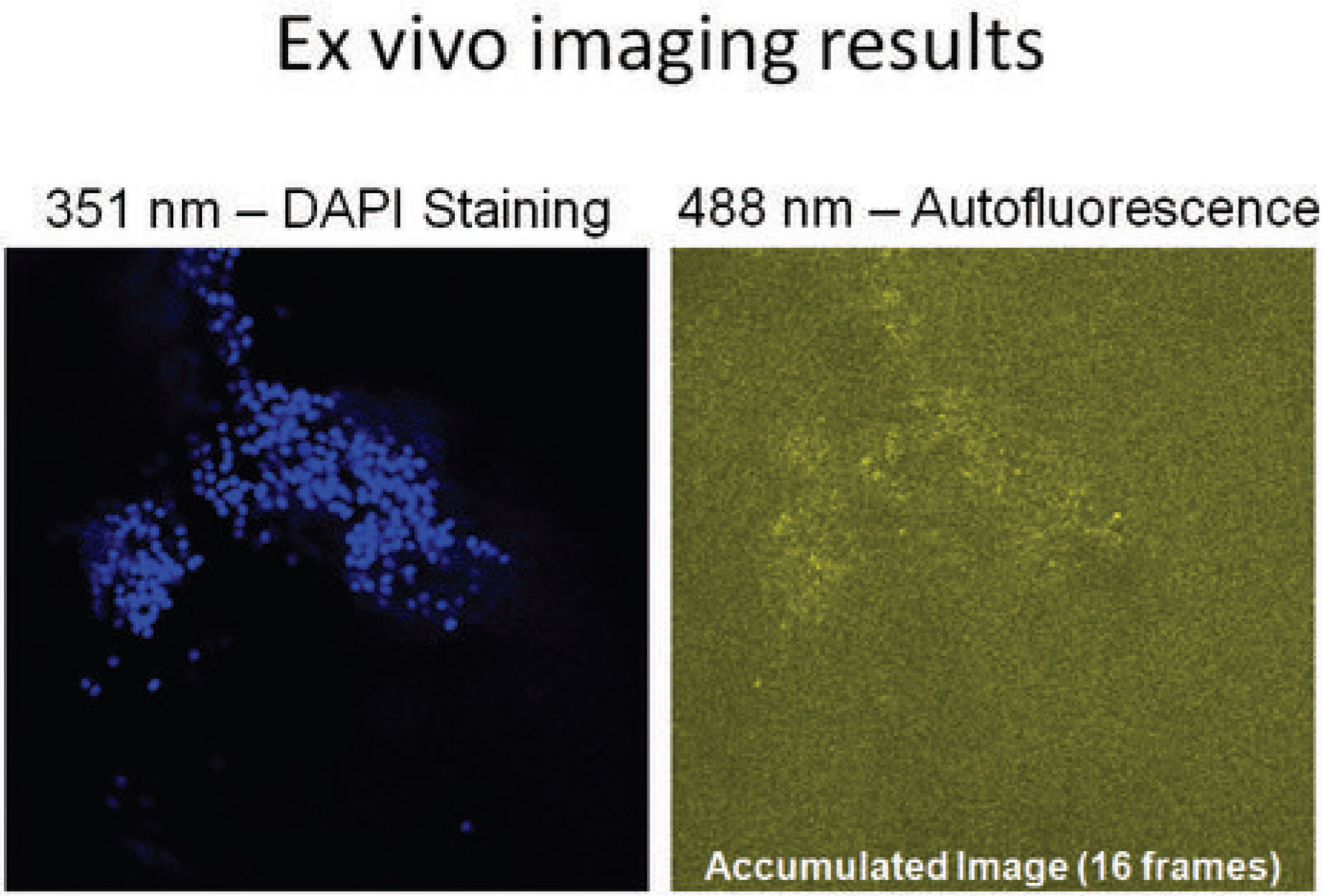

Figure 5. Representative autofluorescence of CA46 B-cells ex vivo

The Balb/C mouse eye was excited with 351 nm light to identify injected CA46 B-cells floating within the aqueous. Excitation of the field with 488 nm light demonstrated successful detection of autofluorescence signals from the same population of cells.

Table 1

Autofluorescence Intensity Ratios By Cell Population and Time

	Resting T-cells (t = 0 days)	CA46 (t = 0 days)	Resting T-cells (t = 1 day)	CA46 (t = 1 day)
445/465	0.81 ± 0.04	0.97 ± 0.02	0.91 ± 0.02	0.99 ± 0.01
445/520(458)	1.05 ± 0.09	0.56 ± 0.04	0.93 ± 0.08	0.69 ± 0.01
465/520(458)	1.31 ± 0.18	0.57 ± 0.04	1.02 ± 0.11	0.70 ± 0.01